NGR-05 – 002-105

DEBYE-SCHERRER INVESTIGATIONS OF EXPERIMENTALLY SHOCKED SILICATES

N71-17178

TMX-66703

Friedrich Hörz

Lunar Science Institute

Houston, Texas

and

William L. Quaide

NASA-Ames Research Center

Moffett Field, Calif.

LUNAR SCIENCE INSTITUTE CONTRIBUTION NO. 02

OUTLINE

ABSTRACT:

Small ballistic ranges were used to perform controlled laboratory shock experiments on 12 selected silicates [quartz (30-310 kb), oligoclase (30-340 kb), andesine (40-100 kb), olivine (80-500 kb), forsterite (50-150 kb), enstatite (60-150 kb), biotite (10-90 kb), hornblende (50-150 kb), garnet (40-160 kb), kunzite (60-150 kb), beryl (60-140 kb), topaz (60-150 kb)]. At least 4 pressure points per mineral are available.

Debye-Scherrer investigations of shocked materials revealed a gradual lattice breakdown of crystalline matter under shock. Individual mineral species behave selectively. Sheet silicates break down very easily, followed by tecto silicates. Chain-, ino- and ortho-silicates are of considerably higher shock resistance. Depending on the mineral species, the first sign of shock damage is evidenced in the long range order at 20-70 kb. At intermediate pressures (100-200 kb) the long range order is essentially destroyed with the short range order heavily disturbed. At pressures exceeding 300 kb tecto silicates are completely collapsed. The degree of internal fragmentation is strongly related to shock pressure, thus providing a sensitive tool for absolute pressure calibration of shocked materials.

The internal fragmentation is structurally controlled, leading to polycrystalline aggregates of strongly preferred orientation. The grain size distribution of the fragmentation products is highly heterogeneous. The mechanisms leading to fragmentation as evidenced by the x-ray patterns are highly complex. The formation of high pressure polymorphs is discussed.

Though application of the new results to naturally shocked rocks may have some limitations, the usefulness of Debye-Scherrer investigations in the study of shocked materials is demonstrated.

INTRODUCTION:

Shock waves in solids are characterized by pressures of high amplitudes and exceptionally short duration, coupled with high temperatures. Materials traversed by such waves such as minerals from nuclear and high-yield chemical explosion sites, meteorite impact craters, some meteorites and laboratory experiments, therefore, have been strained and heated at extreme rates. Accordingly, they contain unique deformation features, partial or complete breakdown of the crystal structure, high pressure polymorphs and melted phases.

Study of the various diagnostic shock phenomena during recent years has lead to the recognition of an empirical sequence of relative shock pressure histories in coexisting mineral assemblages. Various "stages of shock metamorphism" related to progressive peak pressures have been differentiated (STÖFFLER, 1966, CHAO, 1968, DENCE, 1968, v. ENGELHARDT and STÖFFLER, 1968, ROBERTSON et al., 1968, FRENCH and SHORT, 1968). These investigations have been based mainly on optical studies of tecto-silicates. Information regarding other mineral species is only fragmentary. Laboratory shock loading experiments by HÖRZ (1968) and MÜLLER and DEFOURNEAUX (1968) have provided information necessary to calibrate the existing quartz data in terms of absolute pressures. Thus, it is possible to qualitatively evaluate the pressure

histories of siliceous rocks on the basis of optical properties of the component grains only.

DACHILLE et al. (1964) and LIPSCHUTZ and JAEGER (1966) were the first to study shocked materials using x-ray diffraction techniques. They interpreted streaky powder patterns in terms of shock induced disorder. A summary of subsequent work by Lipschutz and his co-workers in meteoritic materials using Debye-Scherrer technique is given by LIPSCHUTZ (1968). BUNCH et al. (1968), CHAO (1968) and SHORT (1969a) discovered identical patterns in shocked quartz. SHORT (1969b) reports them also from olivine and DACHILLE et al. (1968) from quartz, feldspar and calcite. DACHILLE et al. (1968) called attention to the relationship between peak pressure and shock induced disorder. HÖRZ and AHRENS (1969) verified this relationship in a study of Laue x-ray patterns of experimentally shock loaded biotite.

In order to explore this relationship more thoroughly, a variety of rock forming minerals were shock loaded to known peak pressures and the shock products were studied using Debye-Scherrer x-ray diffraction methods. The purpose of this paper is to present the x-ray techniques used and to discuss the complex nature of shock induced disorder. The usefulness of the Debye-Scherrer method as a tool for pressure calibration is evaluated.

EXPERIMENTAL CONDITIONS:

A. Shock Experiments:

The shock loading experiments were performed using small ballistic ranges at the NASA Ames Research Center and the California Institute of Technology. The NASA facility is described in detail by HÖRZ (1970); the vital parts of the Cal Tech range are listed in HÖRZ and AHRENS (1969). Both guns operate under almost identical conditions: the projectile is accelerated by conventional gun powders and the velocities are obtained by measuring elapsed time between interruptions of He/Ne continuous gas lasers. The velocities are measured to an accuracy of $\pm$ .5% for the NASA facility (digital counters) and to $\pm$ 2% for the Cal Tech facility (photographic record of a high speed oscilloscope). The projectiles are flat, polished metal discs, 17 mm in diameter and 2-3 mm thick. The projectile materials used were brass, aluminum and "Fansteel". These discs were inserted in a "Lexan" holder which was then launched as a "projectile". The metal plate faced the side to be impacted. Some few shots were fired without a metal plate and they are referred to as "Lexan", i.e. a solid plastic slug was used.

The mineralogical target was typically a disc 10 mm in diameter and 1 mm thick, made out of single crystal or polycrystalline materials. Because of the small size of some available crystals, deviations from this standard

target geometry were unavoidable. In the case of beryl
and topaz the diameter of the target was as small as .5 mm.
Biotite could not be machined into round discs; therefore,
squares had to be used (8 mm side length). Olivine (small
crystals) as well as hornblende and kunzite (abundant
cleavage planes) were cut into thin slabs with their
natural (prismatic, irregular) outlines preserved. All
targets, however, were kept 1 mm thick. Each target was
embedded in a pressed pellet of either a pure alkalihalogenide
or mixtures of Fe powder and NaCl (see Table 1). The
alkalihalogenide and the Fe-NaCl mixture were chosen to
match the accoustical impedance of the targets (HÖRZ, 1970).
Consequently, irregular outlines of some targets are not
believed to be of any disadvantage. Upon impact, the
pressed salt pellets functioned not only as impedance
matching media for the assortment of minerals, but also as
momentum traps since their low tensile strength caused them
to spall very readily (HÖRZ and AHRENS, 1969). After impact,
the mixture of broken salt and target was collected and the
salt was dissolved in H_2O. For the Fe-NaCl mixtures, a 5
minute 10% HCl leach was sufficient to dissolve the iron
powder. A variety of x-ray tests on hornblende did not
reveal any alterations due to the leaching procedure. The
recovered silicates were fine grained powders with an
average grain size in the .5 to 1 mm range.

B. Pressure Calibration:

The calculation of peak shock pressure is only ap-
proximate for a number of minerals studied. In the case
of quartz and feldspar the pressures were obtained by
graphical impedance match solutions (McQUEEN and MARSH,
1960) using the existing single crystal equation of
state data of WACKERLE (1962) and AHRENS et al. (1969a).
No equation of state data are available for single crystals
of the other minerals investigated. Thus, a variety of
approximations had to be used to calculate the peak shock
pressures.

The pressures for olivine and forsterite were ob-
tained using the equation of state data for dunite (Twin
Sister Peaks, Washington, 92% olivine, McQUEEN et al.,
(1967). The enstatite pressures are based on the equation
of state for bronzitite [Stillwater Complex, Transvaal,
94% pyroxene (90 mol % enstatite), McQUEEN et al., 1967].

The calculation of peak pressures for the remaining
mineral species is even more approximate. Neither single
crystal nor "rock" equation of state data exist for these
materials. The following procedure was used to obtain
the experimental shock pressures: when plotted in the
pressure-shock velocity plane (= Hugoniot-curve) both slope

and shape of equations of state are a function of $d_o U_s$ (d_o = density of unshocked material, U_s = velocity of shockwave). Since U_s equals V_p (= compressional sound velocity) at ambient pressure, a slope of tan $d_o V_p$ matches the unknown equation of state rather closely at low pressures so long as U_s is not considerably larger than V_p. Therefore, a straight line with a slope of tan $d_o V_p$ was used to extrapolate the peak pressures of the remaining mineral species. Pressures up to 70 Kb were read directly off the line. For higher pressures in the 70-150 Kb range, the direct "line" value was increased by 3% (70-100 Kb range) and 6% (100-150 Kb range), thus taking the increasing shock velocities with progressive peak pressures into account. An increase by 3% and 6% respectively was suggested by treating the acoustical data of Twin Sister dunite (McQUEEN et al., 1967) in exactly the same way and comparing these results with those based on the known equation of state data. Most of the sound velocities used were obtained from BIRCH (1966). If no direct measurements were available, the velocities were approximated using an extrapolation scheme for V_p via bulk density and mean molecular weight (BIRCH, 1961, ANDERSON, 1967). The equation of state data for the projectile materials were obtained by ISBELL et al.,

(1966) for Lexan (= polycarbonate plastic), JONES et al.,
(1965) for "Fansteel 77" (= 90% W, 6% Ni, 4% Cu), THIEL
(1966) for Aluminum 2024 (93% Al, 4.5% Cu, 2% Mg) MCQUEEN
and MARSH (1960) for brass (61.5% Cu, 35.2% Zn, 3.2% Pb).

In summary, three different approaches were used to
arrive at graphical solutions of the experimental peak
pressures:

1) Equation of state data for <u>single crystals</u>.

2) Equation of state data for <u>rocks</u> of essentially
    monomineralic composition.

3) <u>Approximation</u> of the equation of state via
    acoustical parameters.

The pressures given in this paper vary accordingly in
their precision. The accuracies are believed to be ± 5%
for the single crystal data, ± 10% for the rock data and,
conservatively, ± 30% for the approximated values. In
order to permit revision of estimated pressures once corre-
sponding single crystal equation of state data become
available, the experimental conditions for shots requiring
approximated pressure solutions are listed in Table 1.

As mentioned earlier, the mineralogic targets were
embedded in alkalihalogenides or a mixture of Fe powder
and NaCl. The embedding media were selected according to
identical considerations as outlined for the pressure

- 8 -

calculations; the object being a close acoustical impedance
match. If possible, a pure compound was preferred. The
percentages of Fe and NaCl respectively were determined for
each individual shot to match the shock velocities of target
and salt pellet at the anticipated pressure levels. The
equation of state data for Fe (McQUEEN and MARSH, 1960) and
NaCl (THIEL, 1966) were used in these calculations.

C. Minerals Investigated:

The minerals subjected to the shock loading experiments
were carefully selected single crystals (with few exceptions).
All were extremely fresh, some even of gemstone quality.
They were selected to cover a wide range of densities and a
variety of silicate structures in order to arrive at some
general conclusions regarding the shock behavior of silicates.
Data pertinent to these studies are described below. Some
chemical microprobe analyses are listed in table 2.

Quartz: Single, untwinned crystal of optical quality;
                 Arkansas. Optical investigations of the
                 shock materials used in this study have been
                 extensively described by HÖRZ (1968),
                 Density: 2.65 gr/cc.

Oligoclase I: Muskwa Lake, Ontario, Canada. Extremely
                 fresh, almost water clear, very regular

twins with twin lamellae being roughly

1 mm wide; three (3) experiments reported

here, i.e. 31 Kb, 48 Kb, and 92 Kb. Density:

2.63 gr/cc.

Oligoclase II: Mitchell Co., North Carolina, very fresh,

almost water clear, coarse albite twins.

All experiments higher than 92 Kb. Density:

2.625 g/cc.

Anorthosite: San Gabriel Mountains, California

(= andesine) very coarse grained (2-5 mm)

irregular feldspar aggregate. Density:

2.68 g/cc.

*Olivine I: St. John's Island, Red Sea. Small but

almost gemstone quality crystals with platy,

prismatic habit.   Four experiments

reported here: 80 Kb, 108 Kb, 145 Kb, and

210 Kb. Density: 3.31 gr/cc.

Olivine II: San Carlos, Arizona. Glassy clear, high

quality single crystals of centimeter size

from olivine clots in basic lava.

Experiments above 210 Kb. Density: 3.35 g/cc.

*Courtesy of E.C.T. Chao, U.S.G.S., Washington, and W.

Weiskirchner, University of Tübingen, Germany.

Forsterite: Stochiometric Mg SiO_4 with minor contaminations, synthetic. Polycrystalline aggregate of apparent random orientation and an average grain size of about 2 mm, optical quality. Density: 3.14 gr/cc.

**Biotite: Lepidomelane, Bancroft, Ontario. Large, very fresh single crystal. The material used in this study was extensively described by HÖRZ AND AHRENS (1969). Density: 2.98 gr/cc.

Hornblende: No locality available. Large, single, fresh crystal of $\simeq$ 1 x 1.5 x 5 cm size; Density: 3.34 g/cc.

Enstatite: Bamble, Norway. Large, single crystal, very fresh, extreme cleavage. Density: 3.24 gr/cc, see Table 2.

Kunzite: Pala, California. Gemstone quality, pinkish single crystal. Density: 3.17 g/cc.

Garnet: (= Pyrope), no locality available, gemstone quality, single crystal. Density: 3.76 g/cc.

**Courtesy of E.C.T. Chao, U.S.G.S., Washington, D. C.

Beryl: Minas Geraes, Brasilia. Prismatic single crystal, gemstone quality, but with a few, minute cracks. Density: 2.73 gr/cc.

Topaz: No locality available. Small, perfect single crystal, gemstone quality. Density: 3.46 gr/cc. .

The targets were prepared by drilling cores along the desired crystallographic directions and slicing the core with a diamond saw. If small, perfectly prismatic crystals were available, they were directly sliced. The discs were finely polished on both sides. The crystallographic orientations were monitored to $\pm\ 2^{\circ}$ using Laue x-ray techniques.

D. Recovery Products:

The recovery products were typically grains in the 1-2 mm size class at low pressures ($<$ 100 Kb) and somewhat finer aggregates at elevated pressures (.5 to 1 mm). Material shocked to each pressure level exhibits a range of shock damage in spite of all experimental efforts to assure that the target is traversed by a plane wave. The reasons for this behavior are complex and not understood. They are common to all experimental shock metamorphism

studies.   Considerable efforts were necessary therefore,
to select those grains which exhibited the highest shock
damage in each individual experiment, the selection
criteria being type and amount of microdeformations,
birefringence, undulatory extinction, mosaicism, etc.
If no unequivocal optical selection could be obtained,
2-5 grains were selected and x-rayed.   After eliminating
the effects of crystal orientation as described later,
the grain with the highest "damage" was assumed to be
representative for the quoted pressure level.

The reader familiar with the field of shock metamorphism
will miss in this report an optical description of the
recovery products.   Since those data are available at
present in a highly fragmentary way, at best, we purposely
present the x-ray investigations only.

E.   X-Ray Experiments:

Single crystals shocked to progressively higher
pressure levels are internally broken down into smaller
and smaller, i.e. increasing numbers of "mosaic blocks".
Consequently, an ideal single crystal is transformed into
a polycrystalline aggregate.   Thus the x-ray techniques
applicable in the study of shock induced internal frag-

mentation need to be discussed, i.e. the complications

arising from the crystal's orientation with respect to the

incident beam so long as the materials closely resemble

single crystals.

Two techniques have been most commonly used in x-ray

diffraction studies of shock induced structural disorder.

Both use Debye-Scherrer cameras ("powder" cameras), with a

single grain randomly mounted on the tip of a glass fibre.

One keeps the grain fixed with respect to the incident beam;

in the other one, the grain is rotated about an axis normal

to the beam. The "stationary" technique is a modified Laue

procedure where both front- and back reflections are recorded

simultaneously. There is no film "plane" but instead a

circular film casette and x-radiation is characteristic

rather than white. The "rotation" technique is simply

the powder method wherein the sample is a single grain.

Both methods were tested using various types of minerals

to determine which technique yields the most reproducible

patterns. Other things being equal, the reproducibility

is controlled by the orientation of the crystal with respect

to the x-ray beam. All test grains were randomly mounted

on glass fibres. Results are illustrated in fig. 1-4.

It can be seen from fig. 1 and 2 that the "rotation"

technique gives the more reproducible patterns because the probability for diffraction by each set of planes is increased. Not only are a number of individual reflections completely missing in the "stationary" patterns (fig. 1), but sometimes also all high angle back reflections (fig. 1b). Laue patterns of the same mineral grain are presented in fig. 3.

These preparatory tests demonstrated that the "stationary" technique has two serious disadvantages:

a) the pattern is extremely dependent on the crystal's orientation with regards to the x-ray beam.

b) The narrow film strip in the powder camera intersects only a small proportion of the general diffraction cone. (The patterns in fig. 3 are taken with white x-radiation. Characteristic radiations would make both effects even worse, since fewer and smaller spots would be produced).

Though not extensively illustrated, the Laue patterns also depend heavily on the crystal's orientation with respect to incident beam (see fig. 3). However this method is superior to "stationary" Debye-Scherrer techniques, since the entire diffraction cones are recorded.

Both "stationary" Debye-Scherrer and Laue techniques
would be meaningful only if a suite of shocked minerals
were precisely oriented parallel to an identical lattice
direction. However, it becomes progressively more difficult
and finally impossible to orient grains which have been
shocked to successively higher pressures, because they
resemble more and more polycrystalline aggregates.

According to these considerations, the "rotation"
technique appears to be the most practical one for
obtaining reliable results. It has good reproducability
for grains shocked to high and intermediate pressures
and the influence of crystal orientation at low shock
levels is partially eliminated. The influence of crystal
orientation in slightly shock forsterite is illustrated
in fig. 4. Eight exposures with different grain
positions were made; fig. 4a and 4c represent extremes,
fig. 4b an "average" of the observed streakiness. Accord-
ingly, at least 3 exposures were made of each slightly
shocked grain.

The amount of streakiness produced is a function of
the mineral's structural state, as will be demonstrated
later. According to general x-ray theory, however,

additional contributing factors are grain size, exposure time, beam intensity and beam diameter. In spite of their importance, these parameters have not been discussed in previous studies of shocked materials.

The influence of grain size on the streakiness of the patterns is considerable, especially in slightly shocked materials where "block" size is large. However, it is our experience that grains differing by up to 25% in size produce essentially identical patterns. In this study therefore, we limited our investigations to the larger grains of a grain size fraction of 0.2-0.315 mm.

The importance of exposure time is graphically illustrated in fig. 5, where Laue patterns of biotite are shown. Quartz grains exposed for 1, 2, and 4 hours using "rotated" Debye Scherrer techniques are illustrated in fig. 6. After 2 hours, the general appearance of the patterns did not change, though subtle changes such as smoothing of some lines could be observed with increasing exposure time. We therefore kept the exposure times for all samples at 4 hours for Cu radiation and 8 hours for the weaker Co radiation as suggested by tests on biotite.

Beam intensity and diameter also influence the observed patterns. "Standard" tubes have a nominal electron target spot of about 12 x 1 mm, "fine focus" tubes of about ₓ8 x .3 mm, while "microfocus" units range in the order of .05 x .05 mm. According to their design, therefore, they differ in beam width and especially in intensity per unit cross-section area, thus resulting in different resolution capabilities. Since we wanted to investigate the effect of as many domains as possible and simultaneously achieve a high degree of resolution, we used fine focus tubes. Investigations performed with "standard" tubes would simulate the same degree of damage at somewhat lower pressures. According to tests on quartz, "standard" tubes lower the pressure level by about 10%; no data can be given for microfocus tubes; however, it is obvious that their increased resolution would reverse this trend.

RESULTS:

A. X-Ray Patterns:

Results of the Debye-Scherrer investigations are shown in fig. 8 through 18. Each sequence is arranged in the same manner. The first two film strips are

unshocked "standard" materials, with the first one being
a standard "powder" pattern and the second one taken from
an unshocked single crystal. The remaining patterns are
taken with single grains which were shock loaded, selected
and x-rayed as outlined earlier.

B. Interpretation of X-Ray Patterns:

Most of the sequences presented in fig. 8 through 18
display basically four phenomena which are explained and
interpreted below. The four phenomena are (fig. 7):

a) Increasing streakiness.

b) Preferred orientation.

c) Line broadening.

d) General reflection trails.

a) Increasing Streakiness:

According to x-ray theory, (GUINIER, 1952, KLUG
and ALEXANDER, 1962), the length and shape of a diffraction
spot is a function of the solid angle formed by the normals
of the diffracting lattice planes. Since this angle is
ideally "o" for a perfect crystal, the resulting spot should
be perfectly small. Due to crystal imperfections in natural
materials, this "solid angle" has a finite size and accord-
ingly a finite diffraction spot. The size of the spots can

increase considerably if external forces cause crystal deformation. The spots become elongated and streaky. The descriptive term "asterism" was initially restricted to streaky, "asterated" Laue front reflection patterns of strained single crystals only (see CULLITY, 1959). It is now widely accepted in describing streaky patterns of all stationary single crystal methods and has even been used to describe patterns obtained using "rotation" techniques. In the latter case however the original definition has been grossly distorted.

According to the "multiplicity" rule (see KLUG and ALEXANDER, 1962) rotated single crystals produce not only one but rather a variety of spots at specific d-spacings. The number of spots depends on the crystal's symmetry and orientation with respect to incident beam.

Both genuine "asterism" and "multiplicity" combined will result in diffraction patterns as seen in "unshocked single grain" and "unshocked powder". Because of the presence and statistical distribution of a large number of crystallites, both factors overlap each other in the powder patterns to merge into smooth Debye rings. The same effects can be observed in the shocked materials: the Debye-Scherrer patterns range from almost undisturbed single crystals to perfect powders. The crystal has been increasingly deformed,

and, more essential new "crystallites" have been generated. The single crystal is internally broken down into more and more "mosaic blocks" of progressively smaller size. We see the transition from a single crystal into a polycrystalline aggregate.

As outlined above, the formation of Debye rings in shocked materials is both a function of internal strain and number of "blocks". Complicated techniques have been suggested (see KLUG and ALEXANDER, 1962) to separate quantitatively the individual effects of strain and domain size. We have not attempted such an analysis. It requires that the materials be annealed to determine the influence of strain alone. This, however, would interfere with the optical investigations planned. Since the domain size effect is much greater than the influence of strain, we will refer in traditional fashion to "block size" only.

For similar reasons we propose that the term "asterism" be replaced by "streakiness" in the investigation of shocked materials using rotated grains. The influence of newly generated "blocks" exceeds by far the "streakiness" caused by strain alone. The generation of "mosaic blocks" coupled with the multiplicity rule in rotation techniques grossly

distorts the term "asterism". The term "asterism" should
be restricted to patterns obtained by stationary techniques
only.

Reflections in the high angle "back reflection" area
develop pronounced streakiness at lower pressures than do
those in the "front reflection" region (fig. 8 through 18).
The back reflections represent planes of high Miller indices
and thus give information regarding the mineral's structural
state for long range ordering. The front reflections represent
planes of low Miller indices and provide information regarding
the degree of short range order at progressively higher peak
pressures. The long range order breaks down first. The
back reflections gradually fade out and disappear completely
at high pressures (fig. 8, 9, and 11). This again is a factor
of block size. The blocks become increasingly smaller and
proportionally more and more are beyond x-ray resolution (see
KLUG and ALEXANDER, 1962). This happens for the front reflec-
tions at somewhat higher pressures. Finally, at a certain
pressure, the whole crystal is broken down into a polycrystalline
aggregate with domain sizes below the limit of coherent
diffraction (fig. 8, 9).

Fig. 8 through 18 and especially 8, 9, and 11 suggest
that increasing streakiness as well as the fading out of

back and front reflections indicate a gradual collapse of
all minerals investigated. The structural breakdown is
closely associated with peak pressure. This correlation
of streakiness and peak pressure provides us with a
sensitive tool to pressure-calibrate shocked materials;
but with the limitations discussed later.

Assuming that the block size effect is vastly greater
than the influence of strain, the following qualitative
statements about block sizes can be made according to
AZAROFF and BUERGER (1958), and CULLITY (1959):

	Pattern Characteristics	Block Size
1)	Few scattered spots	$= 2 \times 10^{-2}$ cm and larger
2)	Many spots, randomly scattered	$= 8 \times 10^{-3}$ to 2×10^{-2} cm
3)	Spots indicate diffraction lines	$= 4 \times 10^{-3}$ to 8×10^{-3} cm
4)	Clearly discernible diffraction lines	$= 10^{-3}$ to 4×10^{-3} cm
5)	Smooth rings, perfect powder pattern	$= 2 \times 10^{-5}$ to 10^{-3} cm
6)	Line broadening, fading out of back reflection	$= 10^{-6}$ to 2×10^{-5} cm
7)	Back reflection missing, diffuse rings	$= 5 \times 10^{-7}$ to 10^{-6} cm
8)	X-ray amorphous	$= 5 \times 10^{-7}$ and smaller

These numbers certainly have to be used with caution.
Internal strain, x-ray absorption coefficient, crystal

symmetry, and other factors also influence the listed

values. However, they give order of magnitude estimates

of block sizes. Preliminary optical investigations indicate

the validity of the above size estimates for shocked

oligoclase.

    b) Preferred orientation:

Another phenomenon of interest (especially in the

front reflection) are lens-shaped streaks and pinching

and swelling rings (see fig. 7 through 18). This is a

phenomenon well known from Debye-Scherrer, but especially

Laue (see fig. 3) investigations of drawn wires or extruded

metal rods (KLUG and ALEXANDER, 1962; CULLITY 1959). Due

to the high stress upon drawing or extrusion, the randomly

distributed metal crystallites rearrange themselves in a

preferred fashion. The crystallites composing the wire

or rod will have preferred orientation which results in

a pinching and swelling of the x-ray diffraction rings.

Phenomenologically we see the same effects in our shock

produced crystallite aggregates.

The mechanisms leading to "preferred orientation" in

the shocked materials are different from those in cold worked

metals, however, a fact which was not always clearly separated in previous shock studies. In the case of metals, in most cases, a fine grained polycrystalline aggregate is deformed; in these shock loading experiments however, we are observing the deformation of a single crystal. The shock induced break up of a single crystal into smaller and smaller domains occurs in such a way that the crystal structure influences the collapse. The individual blocks have not been significantly rotated about their original positions. Thus, "preferred orientation" in shocked materials appears to be a relict of the "host" crystal, rather than a re-arrangement of a random crystallite aggregate.

c) Line Broadening:

At elevated pressures (for quartz and feldspar at about 120 Kb, fig. 8 and 9) a pronounced broadening of the diffraction rings is observed, especially in the back reflection. This phenomenon is again due to internal strain and block size (see CULLITY, 1959). Internal strain in a polycrystalline aggregate causes compressions and tensions at the interfaces of crystallites, thus leading to a genuine shortening or stretching of the theoretical d-spacing. The x-rays are truly diffracted by atomic planes having a

broad distribution of d-spacings about the mean value for
the unshocked material. Since internal strain increases
with pressure, "line broadening" is a function of pressure.
However, line broadening is additionally enhanced by the
decrease in domain size. The more numerous and smaller
the domains become, the more general x-ray scatter is
produced which results also in a broadening of the diffrac-
tion line (KLUG and ALEXANDER, 1962).

Again we are unable to resolve the individual effects of
strain and domain size. Some authors (DACHILLE et al., 1968;
SHORT, 1969b) have used line broadening as a parameter to
estimate different pressure levels. Because of film reading
inaccuracies, however, they pointed out that such results
can only be qualitative at best. We agree with their
findings and conclusions. Reading inaccuracies, the effect
of specimen volume and crystal orientation are sources of
error too difficult to control in Debye-Scherrer work. Line
broadening, however, might develop into a valuable parameter
for pressure calibration if performed with powder techniques
using monochromatic x-rays. A variety of techniques have
been developed in studies of fine grained metals (see KLUG
and ALEXANDER, 1962).

d) General reflection trails:

"Characteristic" x-radiation was used in this study.
Apart from the dominating K_α wave lengths, the beam contains
K_β and "white" background radiation. The reflections caused
by the "continuum" result in sheafs of rays which intersect
the general reflection cones (see BUERGER, 1958). Thus
x-ray patterns of rotated single crystals taken with
characteristic x-ray radiation always contain general
radiation reflection trails. Such trails are typical for
single crystal materials and are not caused by lattice
deformations. They can be enhanced by internal strains,
however, in so far as a range of wave lengths interacts
with a broad range of d values for each set of diffraction
planes.

As illustrated in fig. 7 through 17 the general reflection
trails become broader with increasing pressure, indicating
lattice deformation. At high pressures they become washed
out and finally disappear at very high pressures (see fig.
8 and 9). The intensity and frequency of the trails do not
correlate as systematically with peak pressure as does
"streakiness", because the development of trails has a
strong dependence on crystal orientation. General reflection
trails therefore have not been used for pressure calibration.

The trails nevertheless reveal an important clue to the blocksize distribution of the shocked materials. Because the trails are characteristic for rotated single crystals, their presence in fig. 8 through 18 indicates the existance of large, unstrained and/or strained blocks which are still capable of producing a single crystal pattern. The K_α reflections of these blocks, however, are lost in the Debye rings of the smaller domains. We therefore conclude that the internal fragmentation is highly heterogeneous with respect to block size.

C. Quantitative Evaluation:

The following chapter presents an attempt to quantitatively evaluate the x-ray patterns presented in fig. 8 through 18. Shock induced structural breakdown of individual minerals is probably a highly complicated process and the mechanisms leading to the observed x-ray patterns might be entirely different from mineral to mineral. It is obvious, however, that streakiness is (a) a common feature, and (b) closely associated with peak

pressure. These observations will be used as basis for our
analysis. The authors are open to all criticisms and
comments, aiding in the improvement of such an approach.

Fig. 19 and 20, which relate streakiness and peak shock
pressure, are constructed in the following way: a trans-
parent grid divided into 10 equidistant, horizontal intervals
was superimposed on the original film strips; the grid
width was the same as the film width, (=30mm) i.e. one
interval corresponded to 10% film width (=3mm). Using
this grid, the length of the streaks was measured in mm;
dots and streaks corresponding to identical diffraction
positions were "summarized" by simply adding the length
of each dot or streak. These length measurements were then
normalized with respect to the film width. Thus a diffrac-
tion "line" composed of streaks and dots with a total of
15 mm "length" was 50% of the visible "arc". A complete
Debye-ring was accordingly 100%. These normalized length
measurements are plotted in fig. 19 and 20. Originally
we intended to present such measurements for specific
reflections, but since the orientation of the specimen
influences the length of the streak, the tracing of one
reflection might lead to erroneous results. Consequently,
we averaged over 4 to 6 reflections. The "back reflection"

was read for $\emptyset = 70^{\circ}$ to 80°, the "front reflection" for $\emptyset = 15^{\circ}$ to 25° i.e. at d-spacings of .8217-.7828Å and 2.9785-1.8241Å for Cu radiation, and .9519-.9083 and 3.4559-2.1165Å for Co radiation.

.Though two inaccuracies (reading accuracy, specimen rotation) are inherent in this technique, we believe that fig. 8 through 18 and especially the summarized data in fig. 19 and 20 permit us to pressure calibrate shocked materials conservatively to $\pm$ 20%. This is sufficient for most geological purposes.

It is obvious from fig. 8 through 18 that individual mineral species display the same degree of shock damage at various pressure levels. This is not surprising since the study of naturally shocked rocks has demonstrated that each mineral species breaks down <u>selectively</u> and behaves in its own characteristic way. Quartz and feldspars, for example, are at 350 Kb completely transformed into "diaplectic" glasses (v. ENGELHARDT et al., 1967, = "thetomorphic phases", CHAO, 1967) while pyroxens, hornblende and olivines exhibit essentially no optical evidence of shock deformation. The interaction of various factors, noticeably density, shock impedance and crystal structure (which are closely coupled) are assumed to be responsible for this selective behavior.

The relative ease of structural breakdown is demonstrated in fig. 19 and 20. From fig. 20 it can be seen that biotite breaks down much faster than olivine, etc. It is obvious that the steepness of the back reflection or front reflection bands is a measure of the mineral's resistance to internal fragmentation. In order to facilitate the comparisons, a summarizing plot (fig. 21) is presented by connecting the "o" point in fig. 19 and 20 with the points, where back, and front reflections were characterized by complete rings. This line is representative of the transition from an ordered single crystal to a disordered state where first the long-range order is lost and finally where the short-range order corresponds to a fine grained powder. In some cases where the back (and especially the front) reflection has not reached the 100% of arc level, that position was estimated by extrapolating the average slope of the bands.

The slope of each line is a numerical measure of each mineral's resistance to shock induced fragmentation. However, we refrain from giving numerical values, since the derivations of these slopes contain the summation of all uncertainties inherent in the shock pressure calibration as well as the evaluation of the x-ray patterns. Thus we consider them only as qualitative criteria in the

sense that a decrease in the absolute value of the slope correlates with an increase in shock stability. However, some inconsistancies are apparent (fig. 21): garnet seems to be less stable according to the front reflection criteria than beryl, while this order is reversed in the back reflection. Kunzite too seems to be relatively more stable in the back reflection region. This "reversal" might still be in the region of pressure and reading inaccuracies and demonstrates how careful one has to be in establishing a quantitative relationship between "shock stabilities".

It is established, however, that biotite is less stable than feldspars and quartz, and those, in turn, less stable than pyroxenes, amphiboles, etc. Tecto-silicates are more resistant than sheet-silicates. Chain-silicates, ino-silicates, and ortho-silicates are even more stable. The present investigations do not permit more precise statements; however, they demonstrate that rock forming chain- and ortho-silicates have very similar shock stabilities. With the exception of biotite, these "stabilities" correlate well with optical investigations. According to microscopic investigations of naturally shocked rocks, biotite seems to be a rather stable mineral. This apparent discrepancy

results from the fact that biotite deforms by gliding along
(001) with great ease; however, only small gliding distances
are necessary to produce a "disturbed" x-ray pattern while
still preserving the gross optical properties (HÖRZ and
AHRENS, 1969).

DISCUSSION:

a) "Fragmentation":

Single crystals subjected to shock waves are broken into
small block sizes. The internal fragmentation of materials
shocked to successively higher pressures is evidenced by
increasing streakiness and the fading out of back and
front reflections. Additional evidence of fragmentation
is presented by genuine line broadening. The first signs
of fragmentation occur at pressures where no obvious
optical shock criteria can be detected. The structural
collapse seems to be gradual over a wide pressure range.
The size-frequency distribution of the blocks is heterogeneous.
The ever decreasing size of the blocks can finally reach a
level where it is beyond coherent x-ray diffraction. The
material has become x-ray amorphous and optically isotropic,
i.e. a diaplectic glass. The essential part is that all
these phenomena are solid state reactions. No other geologic
process but shock is known to cause such a solid state

transition from crystalline to x-ray amorphous phases in the materials investigated.

Additional evidence for internal fragmentation is also derived from optical studies and refers to "mosaicism", i.e. fragmentation of minerals in a microscopic scale. Especially CARTER et al. (1968), demonstrated increasing mosaicism in their artifically and naturally shocked olivines and pyroxenes. DACHILLE et al. (1968) used the dispersion of the optic axis in individual quartz grains to support the conclusions from their x-ray studies. SHORT (1966) and HÖRZ (1969) measured increased "fracture densities" with increased peak pressures which, indirectly, are a measure of the mineral's internal fragmentation. Though these observations measured the internal fragmentation on a microscopic scale, they present additional evidence of decreasing block sizes.

b) Mechanisms of fragmentation:

For simplicity we have discussed the observed progressive disordering of silicates in terms of "fragmentation" and "break down". The actual mechanisms leading to smaller and smaller block sizes can differ vastly from mineral species to mineral species. They certainly include deformations

produced both during the compression and relaxation phases of a transient shock event and thus all deformation mechanisms of cataclastic and intergranular flow (GRIGGS and HANDIN, 1960). The most common mechanisms are fracturing, cleaving, slipping, gliding, twinning and kinking.

All these deformation mechanisms are reported from optical investigations of naturally and experimentally shocked rocks. The few mineral species investigated in detail always display a combination of them [quartz: CARTER (1968), v. ENGELHARDT and BERTSCH (1969); feldspar: STÖFFLER (1967), ROBERTSON et al. (1968), JAMES (1969); olivine: CARTER et al. (1968), MÜLLER and HORNEMANN (1970); biotite: CUMMINGS (1968), HÖRZ and AHRENS (1969); pyroxene: JAMES (1969)]. Information regarding other mineral species is only fragmentary. Consequently, the mechanisms leading to the x-ray patterns observed are highly complicated, and presently not understood in detail. However, because all mechanisms result in smaller and smaller domain sizes, we would like to retain the term "fragmentation" for it is descriptive rather than genetic. Regardless of which deformation mode or combination thereof causes "fragmentation" in individual mineral species, it is basically the effect of the size and number of blocks which are observed in the x-ray patterns.

c) High pressure phases:

Detailed optical investigations and equation of state
data are presently available for quartz only (see FRENCH
and SHORT, 1969). According to this information, the
structural collapse of quartz is even more complicated than
outlined above. The equation of state work of AHRENS and
ROSENBERG (1968) and WACKERLE (1962) indicates the formation
of SiO_2 high pressure phases at 100-120 Kb. According to
HÖRZ (1968) and MÜLLER and DEFOURNEAUX (1968) the so called
"planar features" (CARTER, 1968) begin to develop at these
pressures. Subsequently v. ENGELHARDT and BERTSCH (1969)
proposed that planar features are relaxed high pressure
phases. Thus there is overwhelming evidence that the quartz
structure collapses at $\approx$ 120 Kb to a high pressure phase,
be it coesite, stishovite or some disordered phase, respectively
any combination of these. Adiabatic cooling data (AHRENS and
ROSENBERG, 1968) demonstrate that these high pressure phases
can relax upon pressure release to highly disordered phases
of lower density than the original quartz. In addition,
their data indicate a "2 phase region" from $\approx$120 to $\approx$300 Kb;
at higher pressures, only high pressure phases appear to
exist (= "high pressure region").

According to these considerations, the fading out of back and front reflections is not only a function of continuously increasing fragmentation. It is also caused by proportionally increasing amounts of relaxed high pressure phases which, due to their highly disordered structural state, do not diffract x-rays. We thus see in our x-ray patterns (fig. 8, 120 Kb and higher), the combination of two different effects: continuous decrease in block size of ordered α quartz and increasing amounts of relaxed, x-ray amorphous, high pressure phases. Proportionally more and more material is unable to effectively diffract x-rays.

However, if we look at both processes in more detail, they need not be too different. In order to produce SiO_2 high pressure phases, it is necessary to rearrange the SiO_4 tetrahedra. It is not possible to produce coesite or stishovite (probably also "disordered" high pressure phases) without breaking chemical bonds. Thus, "fragmentation" appears to occur at two different levels: (a) in a "macroscale" generating crystal blocks of n-unit cell dimensions and (b) in a "microscale" causing breakdown of the unit cell itself.

Based on equation of state work, optical investigations and the new x-ray results, we believe that the break up of

quartz under shock conditions occurs in the following way:
up to about 100 Kb the "fragmentation" is entirely due to
the generation of relatively large blocks, but the size
distribution of the blocks is heterogeneous. Small
numbers of domains in the 50-100 $\overset{\circ}{A}$ size class are already
present, probably due to crushing effects of the bigger
blocks. It is this small fraction which collapses at
$\approx$ 120 Kb into sub-unit cell dimension to form high pressure
phases. With increasing pressure, the larger blocks
continue to break up into smaller and smaller sizes while,
simultaneously, the formation of high pressure phases
increases. Upon pressure release these relax largely to
a disordered state and thus no longer diffract x-rays.
At pressures of about 200 Kb, the larger blocks break
down into sizes which are beyond x-ray resolution for
high angle back reflections ($\approx$ 500-1000 $\overset{\circ}{A}$). The fragmen-
tation as well as production of high pressure phases
increases and finally at pressures in excess of 300 Kb,
the entire breakdown process has advanced to unit cell
dimensions, i.e. to the production of high pressure
phases exclusively. The relaxed recovery products are
x-ray amorphous and optically isotropic. They are
diaplectic glasses.

Almost identical conclusions can be derived for feldspar,
using the data of STÖFFLER (1967) and AHRENS et al. (1969a).
AHRENS et al. (1969b) combined the static high pressure work
of RINGWOOD and REID (1969), AKIMOTO and FUJISAWA (1968),
and many others with the equation of state work of McQUEEN
et al. (1967), WACKERLE (1962) and AHRENS and ROSENBERG
(1968). They predicted the existence and properties of a
variety of hypothetical high pressure phases in rock forming
minerals including feldspar, olivine and pyroxene. Conse-
quently the complicated "fragmentation" process, including
both decreasing block-size and increasing production rate
of high pressure phases, probably applies to the vast
majority of silicates.

In summary, a series of very complex processes have
been outlined to illustrate the intricate nature of shock
induced disordering, i.e. "streakiness". Though we cannot
differentiate the individual processes, we maintain that
streakiness is a valid measure of the "net" effects.
It is safe to assume that the same processes leading to our
laboratory results also will be responsible for streakiness
observed in naturally shocked samples. Thus one can
compare our results with those of naturally shocked rocks.
It is in this sense, that we want to propose streakiness
as a valid means of shock pressure calibration.

d) Limitations for pressure calculations:

There are some severe limitations to this method, however, in its application to naturally shocked rocks. Those restrictions are a) overlap with static deformation b) shock propagation in rocks c) recrystallization.

a) Overlap with static deformation:

As mentioned earlier, the breakup of crystalline matter under shock into smaller and smaller blocks is caused by intergranular and cataclastic flow. Thus static and dynamic deformation can only be differentiated by the amount of fragmentation; an overlap of the two deformation methods is obvious.

DACHILLE et al. (1968) subjected mineral powders to static deformation up to 100 Kb. They obtained streaky patterns identical to those produced under shock. However their pressures and especially their strain rates exceeded by far the conditions of normal geological processes. At what pressure level the overlap for each mineral lays is uncertain at present. Quartz and feldspar grains from metamorphic rocks (= granitic gneisses) examined by DACHILLE et al. (1968) have a maximum streakiness which corresponds to a 30 Kb shock level.

We are confident that the degree of streakiness in most common silicates produced by a shock wave of 100 Kb amplitude can be distinguished from that produced by static deformation. If impact occurs in previously undeformed rocks however, it is the authors' belief that the shock wave decay in the target can be traced down to a 30-50 kb level. Thus x-ray streakiness is an especially useful tool to detect shock damage at pressure levels where at present optical investigations fail.

b) Shock propagation in rocks:

The single crystal laboratory shock experiments were arranged to generate a plane shock wave. The shock propagation in a polycrystalline aggregate however is highly complex. Due to rarefactions and reflections on individual grain surfaces, the planarity of shock waves in rocks is highly disturbed. STÖFFLER (1967) and CHAO (1967) outlined some of the problems. KIEFFER (1969) demonstrated that individual grains experience multiple passages of shock waves. This may cause increased fragmentation. Each shock wave, though theoretically weaker than its predecessor, is still capable of increasing the breakdown.

Additionally, laboratory shock experiments can generate "natural" peak pressures but they can not reproduce the

pressure pulse durations of natural impact events. The pressure pulse duration in a natural event might be several orders of magnitude higher. The prolonged compressional state during genuine meteorite impact might cause additional fragmentation.

Consequently - because of multiple wave passages and longer pressure pulse durations - naturally shocked materials might show high degrees of streakiness at relatively low pressure levels. It seems though from fig. 8 (coarsely twinned feldspar), fig. 9 (polycrystalline feldspar), fig. 10 (single crystal "olivine") and fig. 11 (polycrystalline "olivine") that polycrystallinity is only of secondary importance. No estimates can be given for the influence of pressure pulse duration.

The correlation of refractive indices and streakiness in experimentally shocked quartz (HÖRZ, 1968 and present results) and naturally shocked quartz (CHAO, 1968) is in excellent agreement. This indicates that naturally and experimentally shocked materials can be compared phenomenologically and are highly self-consistant. Shock pressures in natural materials inferred from shock experiments might not be absolute. However due to longer pressure pulse durations in a natural event, we believe that the experimental pressures can be considered as maximum values.

c) Recrystallization:

Streakiness calibrations fail where the post shock history of the materials displays signs of recrystallization. Recrystallization causes the "block size" to increase. The resulting streakiness therefore would simulate a lower peak pressure, which however can safely be considered as minimum pressure. The actual peak pressure cannot be reconstructed. Consequently extreme caution is necessary in interpreting shock loaded rocks which are of extreme age or which display evidence of recrystallization.

CONCLUSIONS:

Controlled laboratory experiments on a variety of silicates and the resulting Debye-Scherrer investigations revealed that

1) Crystalline matter shocked to progressively higher pressures breaks up into smaller and smaller block sizes.

2) The fragmentation is gradual over a wide pressure range.

3) The size-frequency distributions of the blocks is highly heterogeneous.

4) The fragmentation is structurally controlled as evidenced by preferred orientation.

5) The degree of fragmentation is strongly related
    to peak pressure.

6) The ease of structural collapse changes with
    increasing order of resistance from sheet- to
    tecto- to chain-ino- and ortho-silicates.

Highly complex processes lead to the x-ray patterns observed.
Processes probably vastly different from mineral species
to mineral species result in the same types of x-ray patterns
thus making a quantitative interpretation regarding the
mechanisms of fragmentation exceedingly difficult. Optical
and x-ray studies on experimentally and naturally shocked
materials (at least for quartz) correlate very well. Though
streakiness is a measure of "bulk" effects only, its
strong correlation with peak shock pressure suggests it as
a valid means of pressure calibrating shocked materials.
Despite the fact that streakiness seems to be an independent
calibration tool, it is strongly recommended that both
optical and x-ray investigations are combined to evaluate
the pressure histories of shocked materials.

LITERATURE:

AHRENS, T. J. and ROSENBERG, J.T.: Shock Metamorphism:
  Experiments on Quartz and Plagioclase. In French,
  B. M. and Short, N.M. eds. Shock Metamorphism of
  Natural Materials, Mono Book Corp., Baltimore (1968).

AHRENS, T.J., PETERSON, C.F., and ROSENBERG, J.T.: Shock
  Compression of Feldspars. J. Geophys. Res. $\underline{74}$,
  2727-2746, (1969a).

AHRENS, T.J., ANDERSON, D.L., and RINGWOOD, A.E.: Equa-
  tions of states of shocked silicates and oxides and
  crystal structures of high pressure phases. Rev.
  Geophys. in press, (1969b).

AKIMOTO, S. and FUJISAWA, H.: Olivine-spinel solid
  solution equilibria in the system $Mg_2 SiO_4$ -
  $Fe_2 SiO_4$. J. Geophys. Res. $\underline{73}$, 1467 (1968).

ANDERSON, D.L.: A Seismic Equation of State, Geophys.
  J.R. Astro. Soc. $\underline{13}$, 9-30, (1967).

AZAROFF, L.V., and BUERGER, M.J.: The Powder Method
  in X-ray Crystallography. McGraw-Hill Book Co.,
  New York-Toronto-London, (1958).

BIRCH, F.: The Velocities of Compressional Waves in Rocks
  ‥ Kilobars, Part 2. J. Geophys. Research, $\underline{66}$,
  2199-2224, (1961).

BIRCH, F.: Compressibility; Elastic Constants. Handbook
of Physical Constants, S. P. Clark, Jr., ed. Geol.
Soc. Am. Memoir 97, Yale University, New Haven,
Connecticut (1966).

BUERGER, M.J.: X-Ray Crystallography. John Wiley and Sons,
Inc., New York, (1958).

BUNCH, T.E., COHEN, A.J., and DENCE, M.R.: Shock Induced
Structural Disorder in Plagioclase and Quartz. In
French, B.M. and Short, N.M. eds. Shock Metamorphism
of Natural Materials, Mono Book Corp., Baltimore (1968).

CARTER, N.L.: Dynamic Deformation of Quartz. In French,
B.M. and Short, N.M. eds. Shock Metamorphism of
Natural Material, Mono Book Corp., Baltimore (1968).

CARTER, N.L., RALEIGH, C.B., AND De CARLI, P.S.: Deforma-
tion of Olivine in Stony Meteorites. J. Geophys. Res.
73, 5439-5461, (1968).

CHAO, E.C.T.: Shock Effects in Certain Rock Forming Minerals.
Science, 156, 192-202 (1967).

CHAO, E.C.T.: Pressure and Temperature Histories of Impact
Metamorphosed Rocks - Based on Petrographic Observations.
In French, B.M. and Short, N.M. eds. Shock Metamorphism
of Natural Materials, Mono Book Corp., Baltimore (1968).

CUMMINGS, D.: Shock Deformation of Biotite around a
        Nuclear Explosion. In French, B.M. and Short, N.M.,
        eds. Shock Metamorphism of Natural Materials, Mono
        Book Corp., Baltimore (1968).

CULLITY, B.D.: Elements of X-Ray Diffraction. Addison
        Wesley Co., Reading-London, (1959).

DACHILLE, F., MAEGHER, E.P., and VAND, V.: Shock induced
        Polymorphism or Alteration in Minerals. Geol. Soc.
        Am. Spec. Paper 82, 40,(1964).

DACHILLE, F., GIGL, P., and SIMONS, P.Y.: Experimental
        and Analytical Studies of Crystalline Damage Useful
        for the Recognition of Impact Structures. In French,
        B.M. and Short, N.M., eds. Shock Metamorphism of
        Natural Materials, Mono Book Corp., Baltimore (1968).

DENCE, M.R.: Shock Zoning at Canadian Craters: Petrography
        and Structural Implications. In French, B.M. and
        Short, N.M., eds. Shock Metamorphism of Natural Materials,
        Mono Book Corp., Baltimore (1968).

ENGELHARDT, W.v., and STÖFFLER, D.: Stages of Shock Meta-
        morphism in the Crystalline Rocks of the Ries Basin,
        Germany. In French, B.M. and Short, N.M. eds. Shock
        Metamorphism of Natural Materials, Mono Book Corp.,
        Baltimore (1968).

ENGELHARDT, W.v., and BERTSCH, W.: Shock Induced Planar

    Deformation Structures in Quartz from the Ries Crater,

    Germany. Contr. Mineral and Petrol., 20, 203-234, (1969).

ENGELHARDT, W.v., ARNDT, J., STÖFFLER, D., MÜLLER, W.F.,

    JEZIORKOWSKI, H., and GUBSER, R.A.: Diaplektische

    Gläser in den Breccien des Ries von Nördlingen als

    Anzeichen für Stosswellenmetamorphose. Contr. Mineral.

    and Petrol., 15, 93-102, (1967).

FRENCH, B.M. and SHORT, N.M. eds.: Shock Metamorphism of

    Natural Materials. Mono Book Corp., Baltimore (1968).

GRIGGS, D.T. and HANDIN, J.W.: Observations on Fracture

    and a Hypothesis of Earthquakes. Geol. Soc. Am. Mem.

    79, 347-364, (1960).

GUINIER, A.: X-Ray Crystallographic Technology. London,

    Hilger and Watts Ltd., (1952).

HÖRZ, F.: Statistical Measurements of Deformation Structures

    and Refractive Indices in Experimentally Shock Loaded

    Quartz. In French, B.M. and Short, N.M. eds. Shock

    Metamorphism of Natural Materials, Mono Book Corp.,

    Baltimore (1968).

HÖRZ, F.: Structural and Mineralogical Evaluation of an

    Experimentally Produced Impact Crater in Granite.

    Contr. Mineral. and Petrol. 21, 365-377, (1969).

HÖRZ, F.: A Small Ballistic Range for Impact Metamorphism
Studies. NASA, T.R. in press, (1970).

HÖRZ, F. and AHRENS, T.J.: Deformation of Experimentally
Shocked Biotite. Am. J. Sci. 267, 1213-1229,(1969).

ISBELL, W.M., SHIPMAN, F.H., and JONES, A.H.: Hugoniot
Equation of State Measurements for Selected Geological
Materials, G.M. Defense Research Laboratories Quarterly
Progress Report No. 1, (1966).

JONES, A.H., ISBELL, W.M., and MAIDEN, C.J.: Measurement
of the Very High Pressure Properties of Materials Using
a Light Gas Gun. G.M. Defense Research Laboratories
Technical Report 65-84 (1965).

KIEFFER, S.W.: Shock wave Propagation through Granular
Quartz, Transact. Am. Geophys. Union, 50, 221,(1969).

KLUG, H.P. and ALEXANDER, L.F.: X-Ray Diffraction Procedures
John Wiley and Sons, Inc., New York (1962).

LIPSCHUTZ, M.E. and JAEGER, R.R.: X-Ray Diffraction Study
of Minerals from Shocked Iron Meteorites. Science,
152, 1055-1057, (1966).

LIPSCHUTZ, M.E.: Shock Effects in Iron Meteorites; a Review.
In French, B.M. and Short, N.M. eds. Shock Metamorphism
of Natural Materials, Mono Book Corp., Baltimore (1968).

McQUEEN, R.G. and MARSH, S.P.: Equation of State of Nineteen Metallic Elements from Shock Wave Measurements to two Megabars. J. Appl. Phys., 31, 1253-1269, (1960).

McQUEEN, R.G., MARSH, S.P., and FRITZ, J.N.: Hugoniot Equation of State of Twelve Rocks, J. Geophys. Research, 72, 4999-5036, (1967).

MÜLLER, W.F. and DEFOURNEAUX, M.: Deformationsstrukturen in Quarz als Indikator für Stosswellen; eine experimentelle Untersuchung an Quarzeinkristallen, Z. Geophys. 34, 483-504, (1968).

MÜLLER, W.F. and HORNEMANN, U.: Shock Induced Planar Deformation Structures in Experimentally Shock loaded Olivines and in Olivines from Chondritic Meteorites, in press (1970).

RINGWOOD, A.E. and REID, A.D.: High pressure Transformation of Alkalialumino Silicates and Alumino Germanates. Earth Planetary Sci. Letters, 3, 38-40, (1967).

ROBERTSON, P.B., DENCE, M.R., and VOS, M.A.: Deformation in Rock Forming Minerals from Canadian Craters. In French, B.M. and Short, N.M. eds. Shock Metamorphism of Natural Materials, Mono Book Corp., Baltimore, (1968).

SHORT, N.M.: Effects of Shock Pressures from a Nuclear Explosion on Mechanical and Optical Properties of Granodiorite. J. Geophys. Res. 71, 1195-1215, (1966).

SHORT, N.M.: Progressive Shock Metamorphism of Quarzite
 Ejecta from the Sedan Nuclear Explosion Crater, NASA-
 Goddard Space Flight Center, Greenbelt, Md. Preprint
 No. X-622-69-537, (1969a).

SHORT, N.M.: Shock Metamorphism of Basalt, NASA-Goddard
 Space Flight Center, Greenbelt, Md. Preprint No.
 X-644-69-117, (1969b).

STÖFFLER, D.: Zones of Impact Metamorphism in the
 Crystalline Rocks of the Nördlinger Ries Krater.
 Contr. Mineral. and Petrol. 12, 15-24, (1966).

STÖFFLER, D.: Deformation and Umwandlung von Plagioklas
 durch Stosswellen in den Gesteinen des Nördlinger
 Ries. Contr. Mineral. and Petrol. 16, 51-83, (1967).

THIEL, M.V.: Compendium of Shock Wave Data. U. S.
 Atomic Energy Commission, Div. Technical Information,
 Lawrence Radiation Laboratory, University of California,
 Livermore, Cal. UCRL 50108, (1966).

WACKERLE, J.: Shock Wave Compression of Quartz. J. Appl.
 Phys. 33, 922-937 (1962).

Insert:
 JAMES, O.B.: Shock and Thermal Metamorphism of Basalt by Nuclear
     Explosion, Nevada Test Site. Science, 166 , 1615-162o,(1969)
 JAMES, O.B.: Jadeite: Shock-Induced Formation from Oligoclase,
     Ries Crater, Germany. Science, loo5-loo8, (1969)

FIGURE CAPTIONS:

Fig. 1)   Quartz, 107 kb, "stationary" Debye-Scherrer
          technique, 4 random orientations of grain 107b,
          Cu-radiation. Note irregularity of patterns,
          especially missing back reflection in fig. 1b.

Fig. 2)   Quartz, 107 kb, "rotated" Debye-Scherrer technique,
          4 random orientations of grain 107b, Cu-radiation.
          Note highly increased regularity of patterns as
          compared to fig. 1.

Fig. 3)   Quartz, 107 kb, Laue technique, front reflection,
          grain 107b, white Cu-radiation. a) approximately
          parrallel to c-axis b) randomly oriented. Possible
          intersections of the general diffraction cone with
          the 30 mm "film strip" in the Debye-Scherrer powder
          camera are indicated and drawn to scale. Note how
          irregular and non representative the "stationary"
          Debye-Scherrer technique can be.

Fig. 4)   Forsterite, 96 kb, "rotated" Debye-Scherrer technique,
          Cu-radiation, 3 random orientations. Note "regular-
          ity" of patterns.

Fig. 5)   Asterated biotite, 39 kb, Laue technique. (Polaroid
          film), front-reflection, Co-radiation. Approximately
          parallel to [001], same orientation in each exposure.
          Note influence of exposure time on asterism.

Fig. 6)   Quartz, 107 kb, "rotated" Debye-Scherrer technique,
          grain 107b, same orientation in each exposure,
          different exposure times. Note influence of
          exposure time.

Fig. 7)   Quartz, 107 kb, "rotated" Debye-Scherrer technique,
          grain 107 b. Note: preferred orientation and
          general reflection trails.

Fig. 8)   Debye-Scherrer diffraction patterns of shocked
          quartz (impact direction $\perp$ (0001), pressure
          accuracy $\pm$ 5%, Cu-radiation). Note increasing
          streakiness, line broadening, fading out of
          front- and back-reflection and preferred orienta-
          tion. All the following sequences are arranged
          in identical fashion. The numbers on the right
          are the calculated peak pressures. "o" represents
          unshocked powder and unshocked single crystal
          materials.

Fig. 9)   Debye-Scherrer diffraction patterns of shocked,
          twinned oligoclase. (impact direction: random,
          pressure accuracy $\pm$ 5%, Cu-radiation). Compare
          with fig. 10.

Fig. 10)   Debye-Scherrer diffraction patterns of shocked
           polycrystalline anorthosite (= andesine).
           (impact direction: random, pressure accuracy
           ± 10%, Cu-radiation).   Compare with fig. 9.

Fig. 11)   Debye-Scherrer diffraction patterns of shocked
           olivine (impact direction: ⊥ (hk0), pressure
           accuracy ± 10%, Cu-radiation).   Compare with
           fig. 12.

Fig. 12)   Debye-Scherrer diffraction patterns of shocked
           polycrystalline forsterite (impact direction:
           random, pressure accuracy ± 10%, Cu-radiation).
           Compare with fig. 11.

Fig. 13)   Debye-Scherrer diffraction patterns of shocked
           biotite (impact direction: ⊥ (hk0), pressure
           accuracy ± 30%, Co-radiation).   Note especially
           line broadening in the back-reflection.

Fig. 14)   Debye-Scherrer diffraction patterns of shocked
           hornblende (impact direction ⊥ (001), pressure
           accuracy ± 20%, Cu-radiation).

Fig. 15)   Debye-Scherrer diffraction patterns of shocked
           enstatite (impact direction ⊥ (hk0), pressure
           accuracy ± 10%, Cu-radiation).

Fig. 16)   Debye-Scherrer diffraction patterns of shocked
           kunzite (impact direction: $\perp$ (001), pressure
           accuracy $\pm$ 30%, Cu-radiation).

Fig. 17)   Debye-Scherrer diffraction patterns of shocked
           garnet (impact direction: $\perp$ (110), pressure
           accuracy $\pm$ 30%, Cu-radiation).

Fig. 18)   Debye-Scherrer diffraction patterns of shocked
           beryl (impact direction: $\perp$ (001), pressure
           accuracy $\pm$ 30%, Cu-radiation).

Fig. 19)   Debye-Scherrer diffraction patterns of shocked
           topaz (impact direction: $\perp$ (001), pressure
           accuracy $\pm$ 30%, Cu-radiation).

Fig. 20)   Relation of streakiness and shock pressure in
           quartz. (See text for construction of figure).

Fig. 21)   Relation of streakiness and shock pressure in
           selected silicates. (see text for construction
           of figures).

Fig. 22)   Resistance to structural breakdown under shock of
           various silicates as extrapolated from fig. 21.
           The steeper the slope, the more susceptible to
           fragmentation. (Abscissa represents percent of arc).
           (Bi = biotite, O = oligoclase, A = anorthosite,
           Q = quartz, Be = beryl, E = enstatite, T = topaz,
           H = hornblende, OL = olivine, G = garnet, F =
           forsterite, K = kunzite).

Fig. 23)   Relation between slopes of back reflection

(= $\tan\alpha$) and front reflection (= $\tan\alpha'$).

Abbreviations see fig. 22.

TABLE CAPTIONS:

TABLE 1)   Experimental conditions for shots of problematic

pressure calculations.

TABLE 2)   Chemical microprobe analysis of some materials

used in these studies (courtesy of Dr. A. Albee,

California Institute of Technology, Pasadena).

TABLE 1: Experimental conditions for shots of problematic pressure calculations.

Shot Nr.	Mineral	Impact Direction (± 2°)	Projectile Material	Impact Velocity m/sec.	Imbedding Medium	Final Shock Pressure kb
8	Biotite	(001)	Lexan	388	NaI	10 ± 30%
2	"	"	Brass	565	"	39 "
151	"	"	"	872	"	65 "
150	"	"	"	1072	"	86 "
17	"	(hk0)	Lexan	370	"	9 "
5	"	"	"	546	"	36 "
148	"	"	"	870	"	65 "
149	"	"	"	1086	"	87 "
167	Hornblende	(001)	Brass	513	Fe/NaCl	65 ± 20%
168	"	"	"	680	"	90 "
169	"	"	"	835	"	112 "
170	"	"	"	1018	"	140 "
162	Kunzite	(001)	Brass	498	Fe/NaCl	63 ± 30%
163	"	"	"	710	"	93 "
164	"	"	"	870	"	117 "
165	"	"	"	1062	"	150 "

TABLE 1
Page 2

Shot Nr.	Mineral	Impact Direction (± 2°)	Projectile Material	Impact Velocity m/sec.	Imbedding Medium	Final Shock Pressure kb	± 30%
138	Garnet	(110)	Brass	520	Fe/NaCl	74	± 30%
139	"	"	"	665	"	96	"
140	"	"	"	904	"	141	"
141	"	"	"	1042	"	165	"
134	Topaz	(001)	Brass	512	Fe/NaCl	65	± 30%
135	"	"	"	627	"	82	"
136	"	"	"	750	"	102	"
137	"	"	"	1050	"	147	"
144	Beryl	(001)	Brass	502	KBr	60	± 30%
145	"	"	"	715	"	86	"
146	"	"	"	850	"	103	"
147	"	"	"	1080	"	136	"

TABLE 2: Chemical microprobe analyses of some materials used in these studies (courtesy of A. Albee, California Institute of Technology, Pasadena).

	SiO_2	Al_2O_3	FeO	MnO	MgO	CaO	Na_2	K_2O	Total
Oligoclase, Muskwa Lake, Canada	63.9	22.6	.07	---	0.02	4.3	9.2	.4	100.5
Oligoclase, Mitchell Co.	65.7	21.7	---	---	---	3.0	9.4	.3	100.1
Olivine, St. John's Island, Red Sea	40.0	.04	9.9	.16	50.7	---	.01	---	100.8
Forsterite, synthetic	42.4	0.05	.02	---	58.8	---	---	---	101.3
Enstatite, Bamble, Norway	56.7	0.01	9.7	---	33.9	.29	---	---	100.6
Lepidomelane, Bancroft, Canada	39.0	10.8	17.8	.89	13.9	---	.53	8.7	93.8*

* 2.21% TiO_2, balance: H_2O (= 6. %)

Fig. 1) Quartz, 107 kb, "stationary" Debye-Scherrer technique, 4 random orientations of grain 107 b, Cu-radiation. Note irregularity of patterns, especially missing back reflection in fig. 1b.
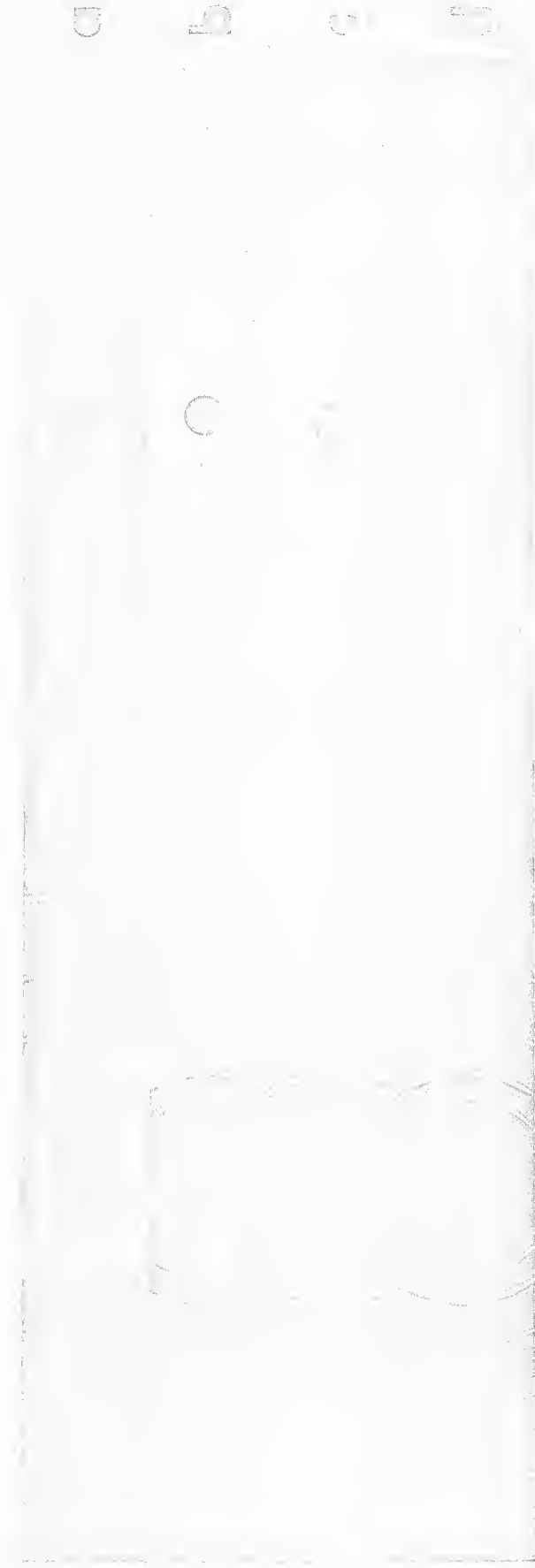
Fig. 2) Quartz, 107 kb, "rotated" Debye-Scherrer technique, 4 random orientations of grain 107 b, Cu-radiation. Note highly increased regularity of particles as compared to Fig. 1.

Fig. 3) Quartz, 107 kb, Laue technique, front reflection, white Cu-radiation, grain 107 b, a) approximately parallel to c-axis; b) randomly oriented.

Possible intersections of the general diffraction cone with the 35 mm "film strip" in the Debye-Scherrer powder camera are indicated and drawn to scale. Note how irregular and non-representative the "station-ary" Debye-Scherrer technique can be.

Fig. 4) Forsterite. 96 kb, "rotated" Debye-Scherrer technique, Cu-radiation, 3 random orientations. Note "regularity" of patterns.
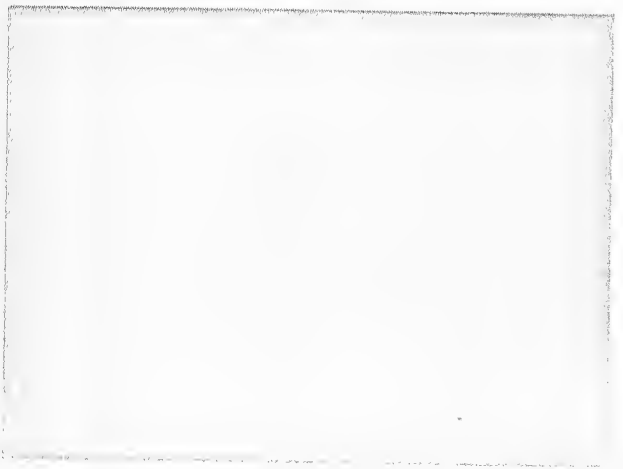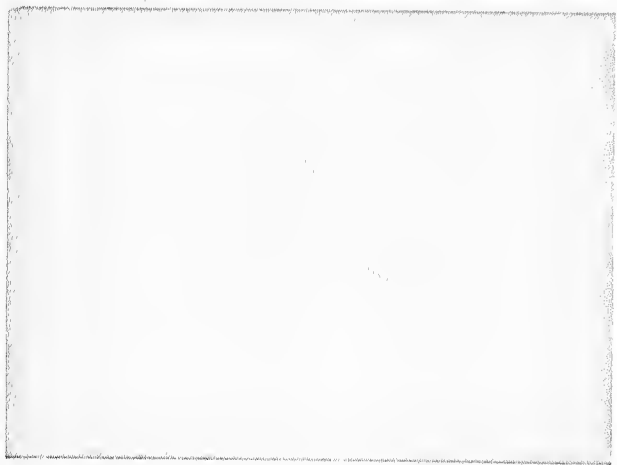
12 min

30 min

8 min
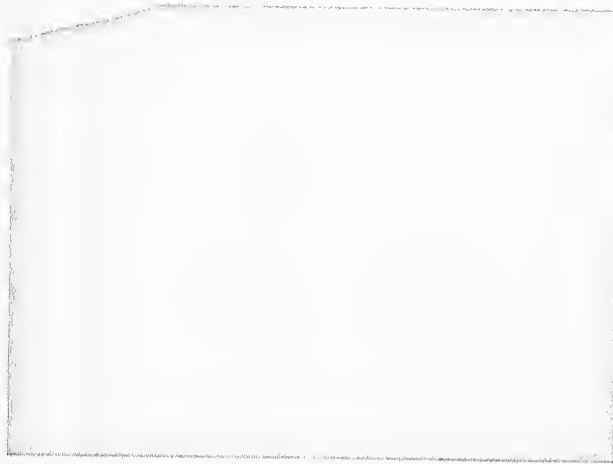
20 min

5 min
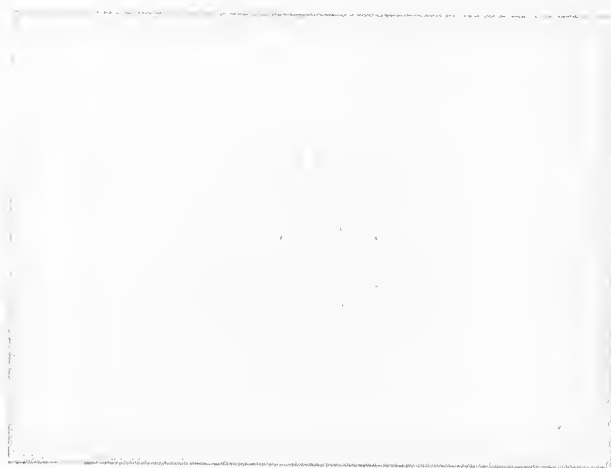
15 min

Fig. 5) Biotite, 39 kb, Laue technique, (Polaroid film), front-reflection, Cu-radiation.
Approximately parallel to [001], same positions. Note influence of exposure
time on length of streaks.

Fig. (c)   Quartz, 107 kb, "rotated" Debye-Scherrer technique, same orientation, grain 107 b, different exposure times. Note influence of exposure time.
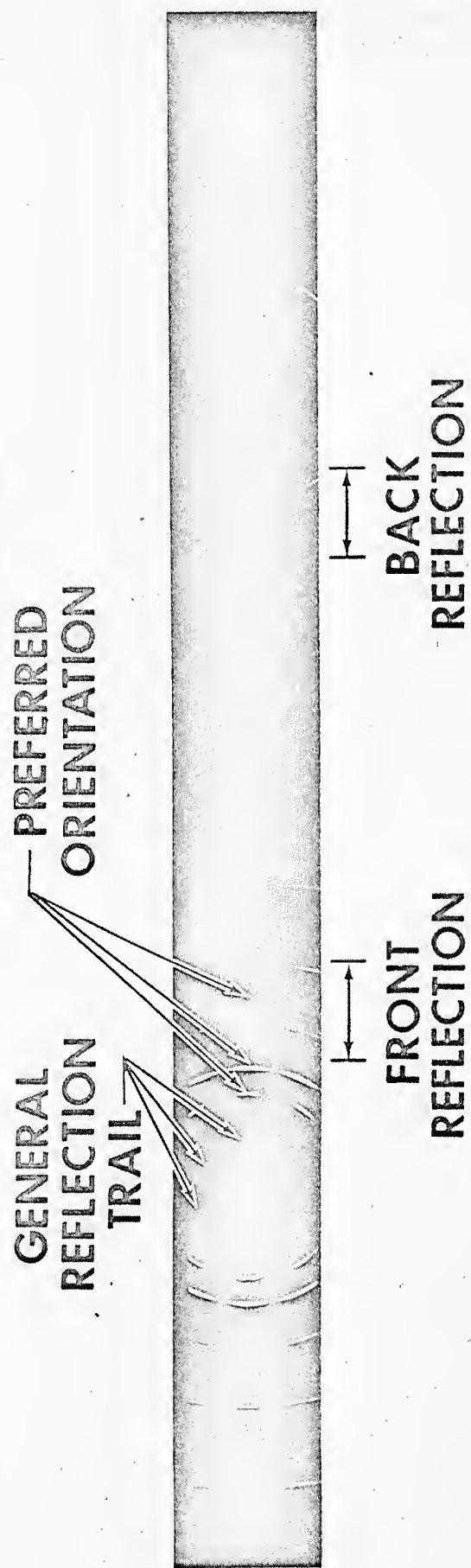
Fig. 7)   Quartz 107 kb, "rotated" Debye-Scherrer technique, grain 107 b.
Note: preferred orientation and general reflection trails.

Fig. 8) Debye-Scherrer diffraction patterns of shocked quartz (Impact direction ⊥ (0001), pressure accuracy ± 5%, Cu-radiation). Note increasing streakiness, line broadening, fading out of front-and back-reflection and preferred orientation. All the following sequences are arranged in identical fashion. The numbers on the right are the calculated peak pressures. "o" represents unshocked powder and single crystal materials.

Fig. 9) Debye-Scherrer diffraction patterns of shocked, twinned oligoclase.
(Impact direction: random, pressure accuracy ± 5%, Cu-radiation). Com-
pare with fig. 10.

Fig. 10)   Debye-Scherrer   diffraction patterns of shocked polycrystalline anorthosite
            (= andesine). (Impact direction: random, pressure accuracy $\pm$ 10%, Cu-radiation).
            Compare with fig. 9.

Fig. 11) Debye-Scherrer diffraction patterns of shocked olivine (Impact direction: ⊥ (hk0) pressure accuracy ± 10%, Cu-radiation). Compare with fig. 12.
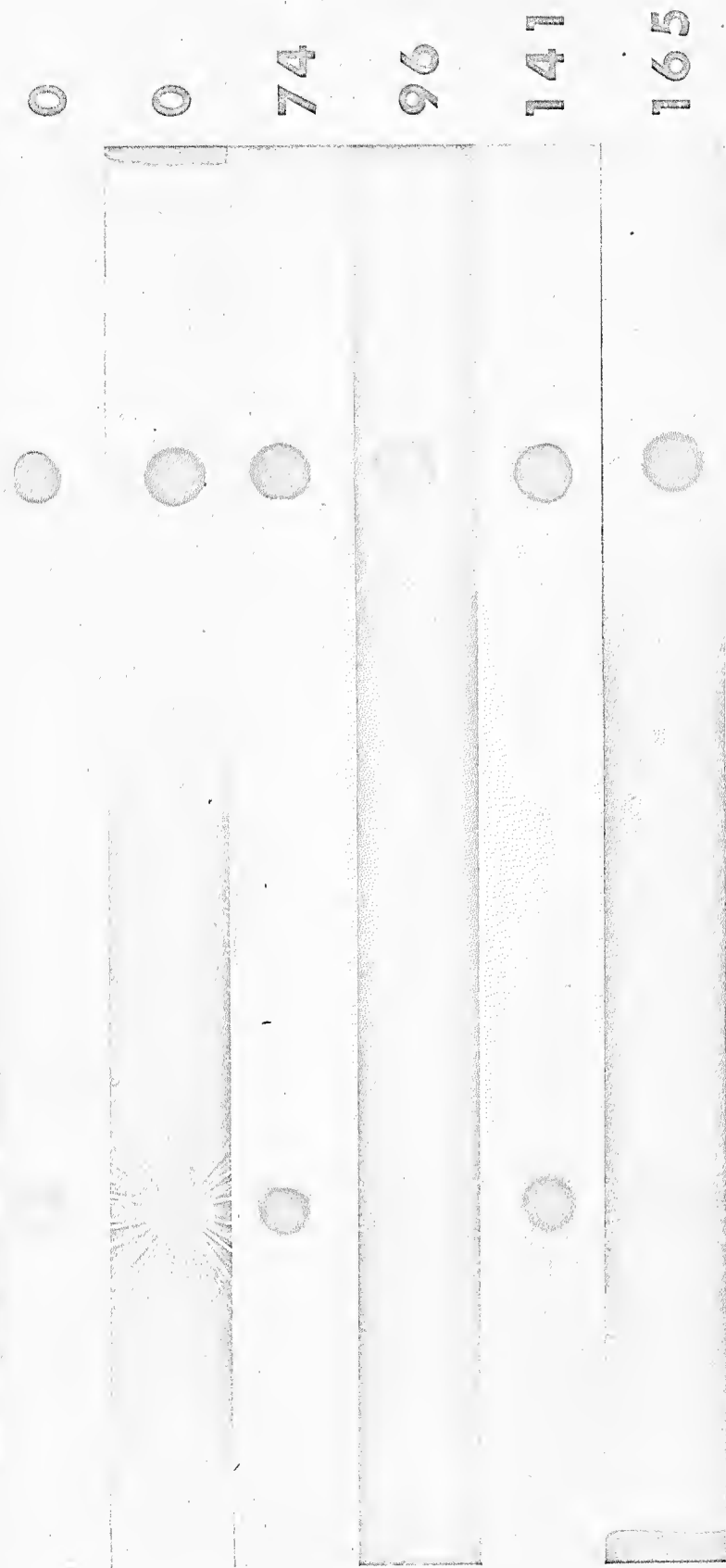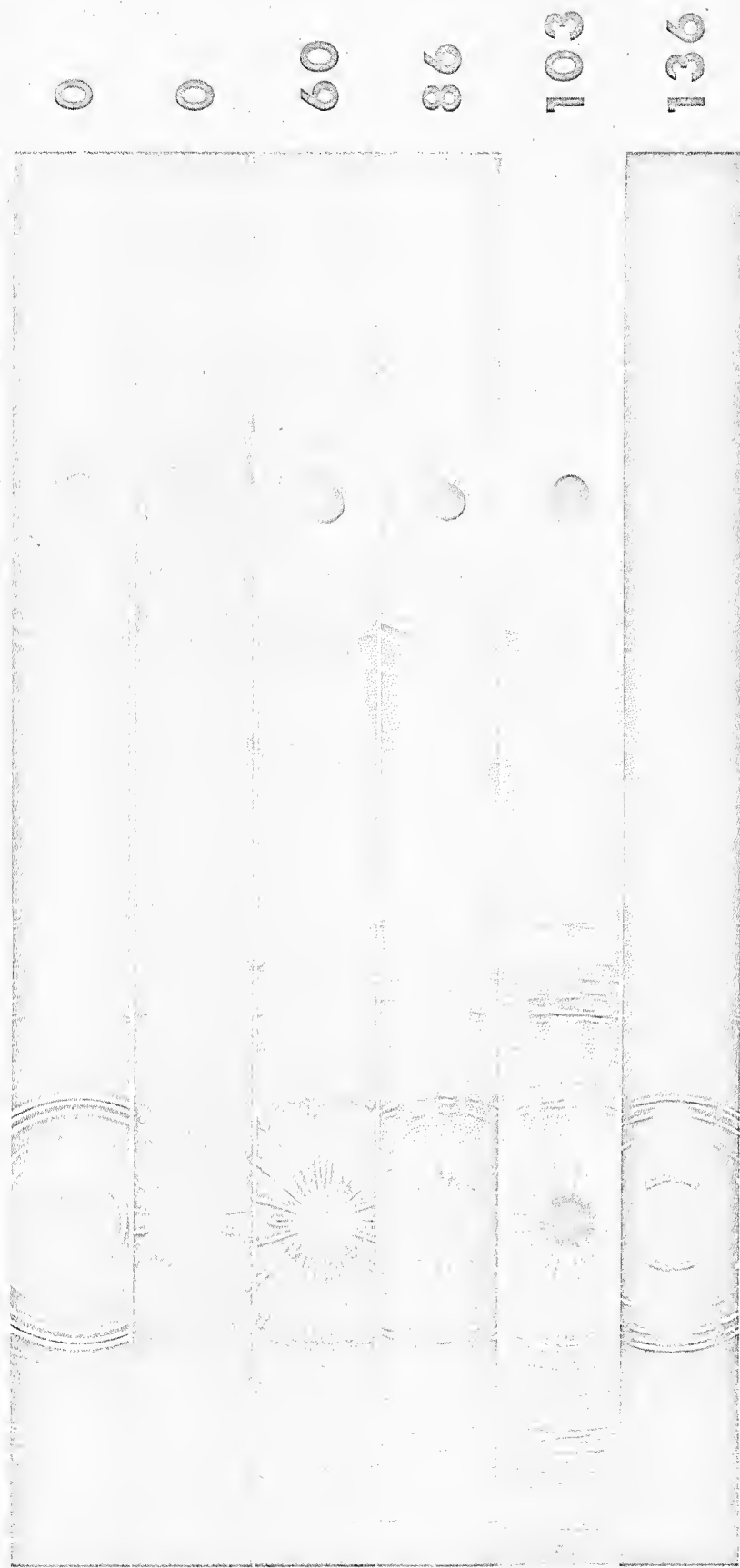
Fig. 12) Debye-Scherrer diffraction patterns of shocked polycrystalline forsterite
(Impact direction: random, pressure accuracy ± 10%, Cu-radiation). Compare
with fig. 11.

Fig. 13) Debye-Scherrer diffraction patterns of shocked biotite (Impact direction:
(hk0), pressure accuracy + 30%, Co-radiation). Note especially line broad-
ening in the back-reflection.

Fig. 14) Debye-Scherrer diffraction patterns of shocked hornblende (Impact direction: ⊥ (001), pressure accuracy ± 20%, Cu-radiation).
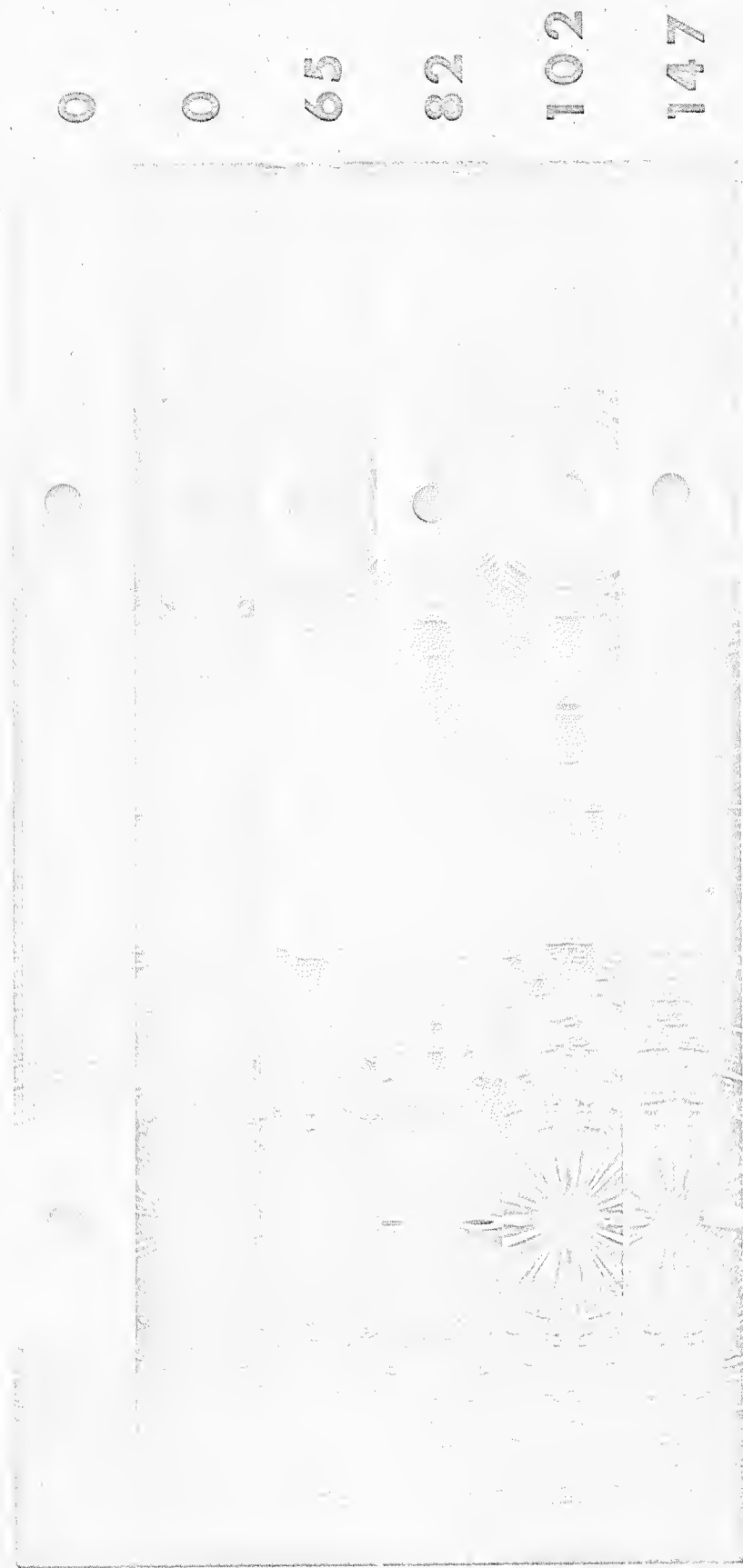
Fig. 15)   Debye-Scherrer diffraction patterns of shock enstatite (Impact direction: ⊥ (hk0), pressure accuracy ± 10%, Cu-radiation).
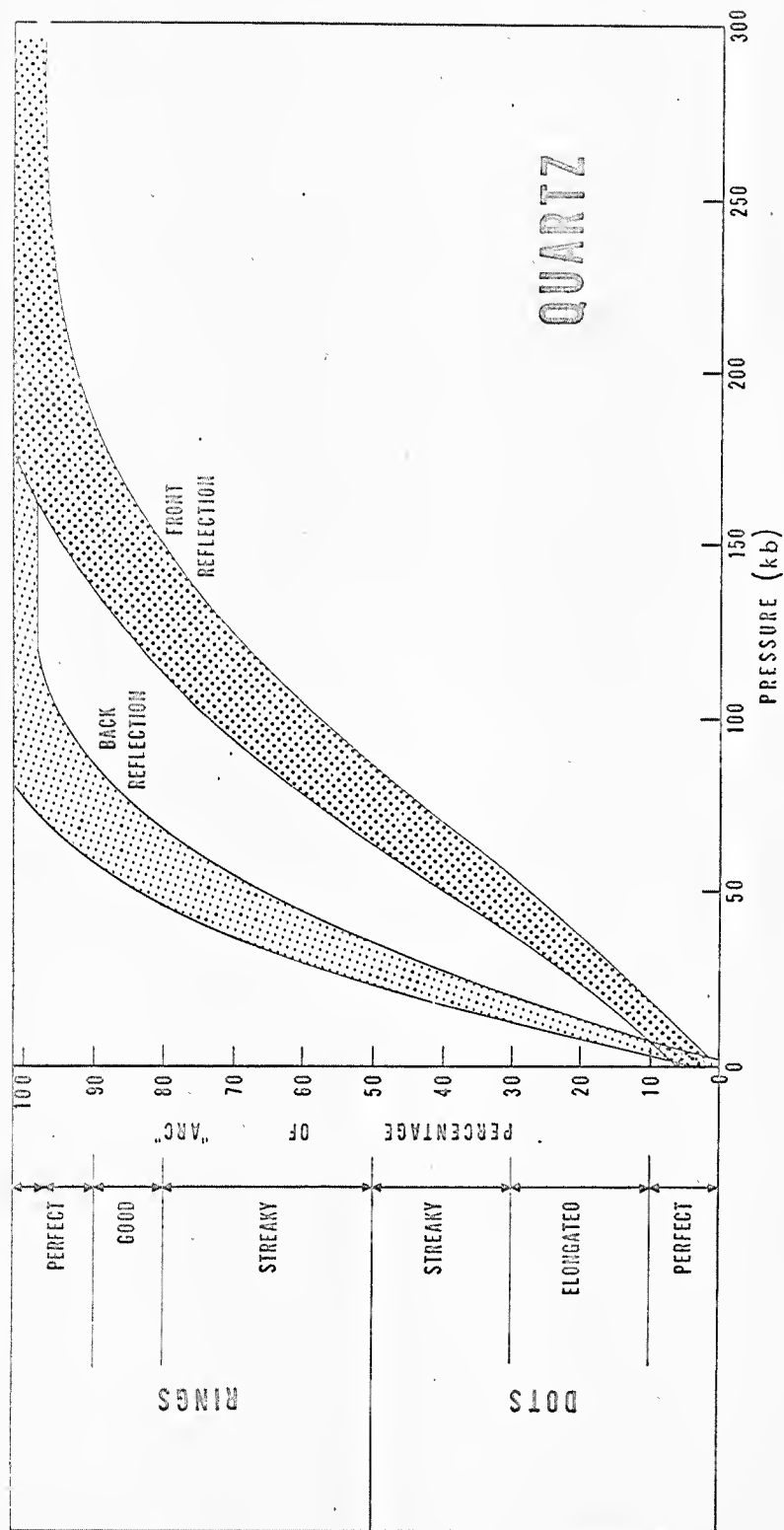
0

0

63

93 .

117

150

Fig. 16) Debye-Scherrer diffraction patterns of shocked kunzite (Impact direction: ⊥ (001), pressure accuracy ± 30%, Cu-radiation).

Fig. 17) Debye-Scherrer diffraction patterns of shocked garnet (Impact direction: ⊥ (110), pressure accuracy ± 30%, Cu-radiation).

Fig. 18) Debye-Scherrer diffraction patterns of shocked beryl (Impact direction: ⊥ (001), pressure accuracy ± 30%, Cu-radiation).

Fig. 19) Debye-Scherrer diffraction patterns of shocked topaz (Impact direction: $\perp$ (001), pressure accuracy $\pm$ 30%, Cu-radiation).

Fig. 20)   Relation of streakiness and shock pressure in quartz   (see text for construction of figure)

Fig. 21 (a) Relation of streakiness and shock pressure in selected silicates. (See text for construction of figures)
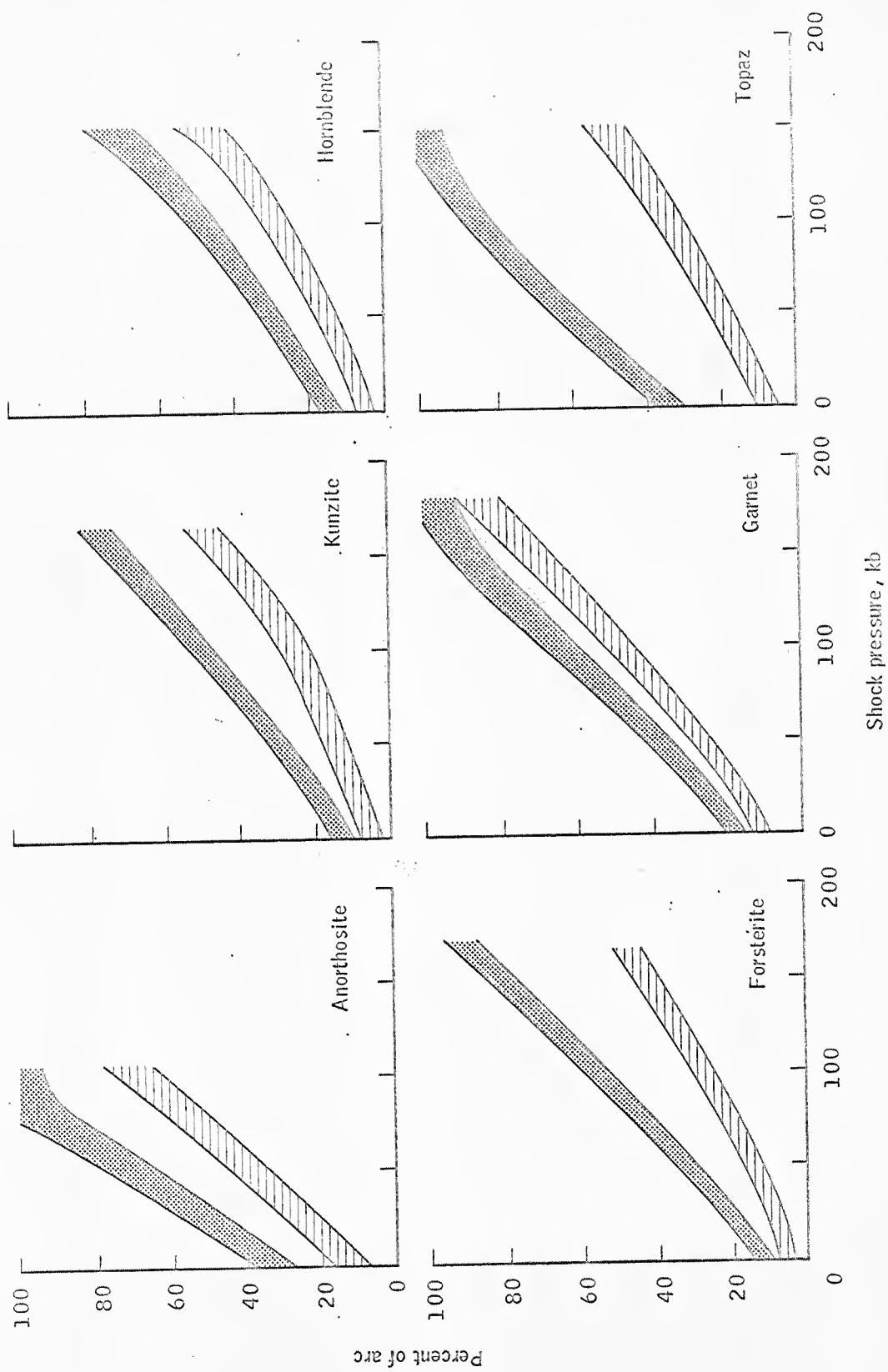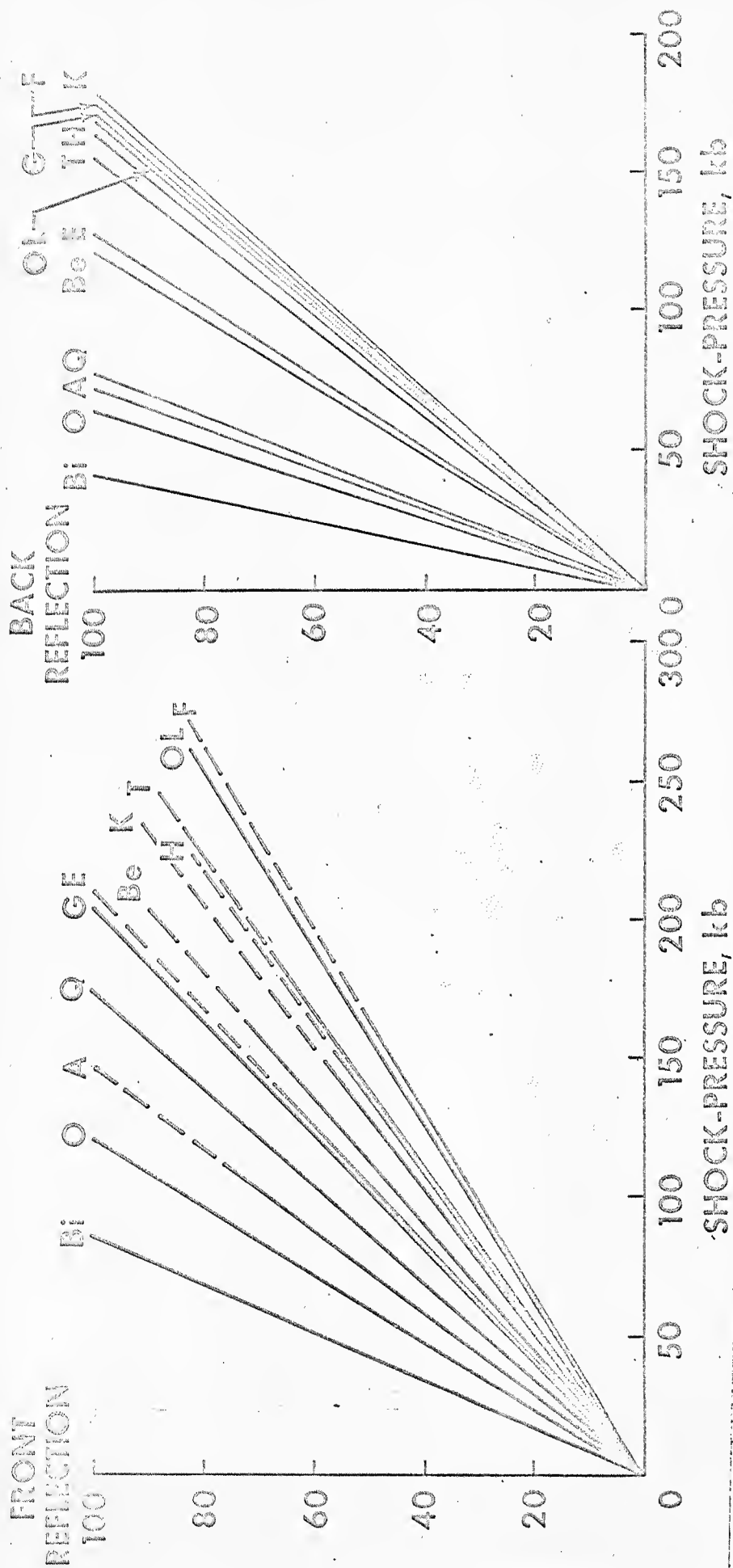
Fig. 21 (b)

Fig. 22) Resistance to structural breakdown under shock of various silicates as
extrapolated from fig. 21. The steeper the slope, the more susceptible
to fragmentation. (Abscissa represents again percentage of arc).
(Bi = biotite, O = oligoclase, A = anorthosite, Q = quartz, Be = beryl,
E = enstatite, T = topaz, H = hornblende, OL = olivine, G = garnet,
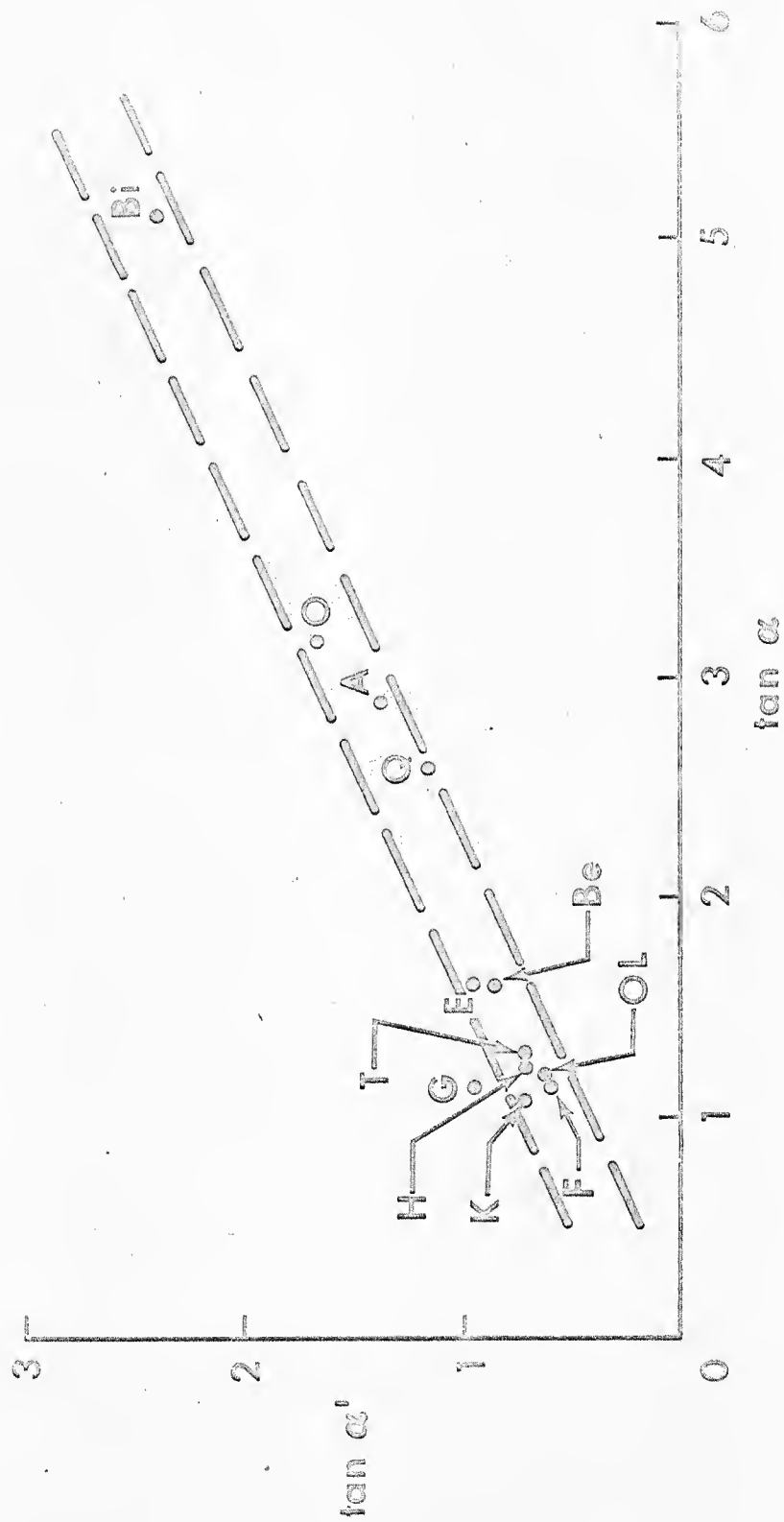F = forsterite, K = kunzite).

Fig. 23) Relation between slopes of back reflection ($= \tan \lambda$) and front reflection ($= \tan \lambda'$). Abbreviations see fig. 22.